

AD-A241 104



REDUCED INTERFERENCE TIME-FREQUENCY
DISTRIBUTIONS: APPLICATIONS TO
ACOUSTIC TRANSIENTS

William J. Williams
Project Director

Electrical Engineering and Computer Science
Systems Division
University of Michigan

Final Report for
ONR Contract
N00014-89-J-1723

DISTRIBUTION STATEMENT A
Approved for public release;
Distribution Unlimited

91-11804



Abstract

A new conceptualization of time-frequency (t-f) energy distributions is discussed in this paper. Many new t-f distributions with desirable properties may now be designed with relative ease by approaching the problem in terms of the ambiguity plane representation of the kernel. Careful attention to the design principles yields kernels which result in high resolution t-f distributions with a considerable reduction of the sometimes troublesome cross terms observed when using other distributions such as the Wigner Distribution (WD). When these new t-f distributions are applied to some common signals, fascinating new details emerge. Examples are provided for joint sounds and marine mammal sounds.

Background

Signals of practical interest often do not conform to the requirements of realistic application of Fourier principles. The approach works best when the signal of interest is composed of a number of discrete frequency components so that time is not a specific issue, (e.g. a constant frequency sinusoid) or somewhat paradoxically, when the signal exists for a very short time so that its time of occurrence is considered to be known (e.g. an impulse function). Much of what we are taught implies that signals that can not be satisfactorily represented in these ways are somehow suspect and must be forced into the mold or abandoned.

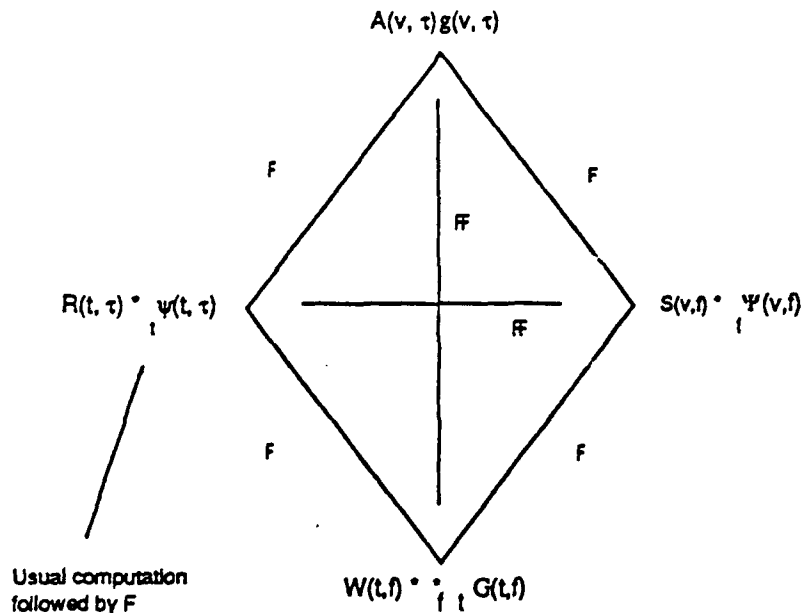
It has been quite difficult to handle nonstationary signals such as chirps satisfactorily using conceptualizations based on stationarity. The spectrogram represents an attempt to apply the Fourier Transform for a short-time analysis window, within which it is hoped that the signal behaves reasonably according to the requirements of stationarity. By moving the analysis window along the signal, one hopes to track and capture the variations of the signal spectrum as a function of time. The spectrogram has many useful properties including a well developed general theory. The spectrogram often presents serious difficulties when used to analyze rapidly varying signals, however. If the analysis window is made short enough to capture rapid changes in the signal it becomes impossible to resolve frequency components of the signal which are close in frequency during the analysis window duration.

The WD has many important and interesting properties. It provides a high resolution representation in time and in frequency for a non stationary signal such as a chirp. In addition, the WD has the important property of satisfying the time and frequency marginals. However, its energy distribution is not non-

negative and it often possesses severe cross terms, or interference terms, between components in different t-f regions, potentially leading to confusion and misinterpretation.

Both the spectrogram and the WD are members of Cohen's Class of Distributions. Cohen has provided a consistent set of definitions for a desirable set of t-f distributions which has been of great value in guiding and clarifying efforts in this area of research. Among the desirable properties are the absence of negativity of the energy values (the spectrogram has this property, the WD does not) and the property of proper time and frequency marginals (the WD has it, the spectrogram does not). A recent comprehensive review by Cohen provides an excellent overview of time-frequency distributions and recent results¹.

Any member of Cohen's Class of distributions can be obtained by combining a kernel with an instantaneous autocorrelation. In the ambiguity plane. Some of the relationships are shown below.



$$W(t, f) = \int x(t + \tau/2) x^*(t - \tau/2) e^{-j2\pi f\tau} dt \quad (\text{Wigner Dist.}) \quad (1)^\dagger$$

$$A(v, \tau) = \int x(t + \tau/2) x^*(t - \tau/2) e^{-j2\pi v\tau} d\tau \quad (\text{Sym. Ambig. Fcn}) \quad (2)$$

[†] All Integrals are over the entire real axis

Many investigators have considered the WD to be the basic t-f distribution. Its principal faults, non-negativity and the cross terms have been considered to be facts of life which can only be dealt with by performing additional computations. Recent developments in our group have convinced us that there are many t-f distributions with properties nearly as desirable as the WD, but with considerably reduced interference terms. Figure 1 illustrates the effect of three choices of kernels, the WD kernel (Figure 1a.), the spectrogram kernel (Figure 1b.) and a new kernel² designed to shape the generalized ambiguity function so as to reduce cross terms (Figure 1c.). The kernel for this distribution is of the form

$$g_r(v, \tau) = \exp(-v^2\tau^2/\sigma) \quad (3)$$

where σ is the parameter to control the amount of interference suppression. We shall discuss distributions in this paper which have kernels with similar characteristics.

Reduced Interference Distributions

Figure 1d. is the ambiguity function of two different frequency sinewave segments occurring at different times. The time domain representation of these two signals is shown in front of the t-f distribution obtained assuming the kernels immediately above them were multiplied by the ambiguity function of the two signals. Computation was in the discrete form. Figure 1e. shows the result obtained using the WD kernel, Figure 1f. shows the result obtained using a possible spectrogram kernel (two-dimensional gaussian) and Figure 1g. shows the results using $g_r(v,t)$. One can see that there are strong interference terms between the two signals in the WD representation. The spectrogram has no cross terms, but the t-f representation is not a faithful representation of the time duration and frequency spread of the two signals. Figure 1g shows a quite faithful representation of the two signals, however. The time and frequency resolution is nearly the same as the WD, but the interference terms are not visible.

A descriptive name has been given to distributions whose kernels possess the four characteristics which lead to the much reduced interference terms. The name Reduced Interference Distribution or RID has been proposed³. The reason that the RID approach is successful can easily be seen by looking at the ambiguity function in Figure 1d. The desired components of the ambiguity function fall near the origin. The interference terms are far from the origin⁴. The WD kernel includes them with equal weight along with the desired terms

because of its unity value. The RID kernel suppresses these interference terms, however, and retains the desired terms.

Figure 2 represents a more ambitious comparison of the WD, spectrogram and RID kernel results. Figures 2a, 2b and 2c show the results for the WD, the spectrogram kernel and the RID. The signal is composed of a chirp plus FM signal. The WD represents the signals well, but strong interference terms are observed between the two signals⁵. The spectrogram represents the chirp fairly well, but the FM signal is very poorly represented, however. The RID result is essentially as good as the WD result for the desired parts of the t-f distribution, but with hardly any interference terms, in sharp contrast to the WD.

The required properties of RID, a list of desirable properties and some distribution comparisons are shown in Tables 1 and 2 the Essential Reduced Interference Distribution Requirements.

Applications

Some comparisons of RID with spectrograms and WDs are appropriate. Figure 3. compares the Spectrogram (a), the WD (b) and the RID (c) for 2 cycles of a sinusoid separated by 2 cycles, 4 cycles 8 cycles and 16 cycles as one progresses from left to right. This is for a 256 point window. Notice that the spectrogram completely misses the on-off of the sinusoidal pulse. It correctly reflects the harmonic structure of the on-off pulsing, however. The WD reflects the harmonic structure in frequency and the time structure as well, but with some breaking up due to interference terms. The RID faithfully reflects the harmonic structure and the time structure. Figure 4 compares spectrogram, WD and RID for an off-on sine with increasing duty cycle time for window lengths of 64 128 and 256 points. The WD and RID perform well here. The WD interference terms are not as evident due to the finite analysis window lengths. The results in Figures 3 and 4 were motivated by Watkin's paper⁶ on limitations of the spectrogram and include recreations of his spectrogram results.

Figure 5. compares spectrogram and RID results for a TMJ click during jaw movement. Figure 6. shows RID results for a bottlenose dolphin. Note the relative invariance of the t-f patterns compared to the time series underneath. The spectrum gives little hint of the t-f structure. Figure 7 shows RID results for spermwhale clicks. Note the repeated triplets in the data from the two hydrophones.

Conclusions

1. RID produces very useful and interpretable results for natural signals. Unique signatures for underwater sounds seem to be an attractive feature and capability of RID.
2. RID well represents what one would conceptually expect from an ideal time-frequency distribution in many situations.
3. The precise time and frequency structure of RID may allow source and multipath structures to be disassociated.
4. Care must be taken in proper computation, display and interpretation of results.
5. There are conditions where the performance of RID is not as good as a specialized distribution or approach designed to the signal and situation.
6. The RID possesses almost all of the desirable properties of a time-frequency distribution and is particularly useful in multicomponent situations where the reduced interference property is very desirable.
7. The Wigner distribution still has an important place in theory and in application, particularly when interference is not an issue, when one desires to use time-varying filtering and synthesis techniques and when signal detection is an issue. It may also be desired if cross terms are useful.

Acknowledgement

We are grateful for the collaboration of the group at Dr. Bill Watkin's Laboratory at WHOI and the marine mammal sounds provided from their database - Dr. Watkins, Dr. Kurt Fristrup and Dr. Peter Tyack.

Author	
Title	
Organization	
Justification	
*Res Lts	
Distribution	
Availability	
Access	
A-1	

References

- 1 L. Cohen, "Time-Frequency Distributions". IEEE Proceedings, July, 1989.
- 2 H. I. Choi and W. J. Williams. "Improved Time-Frequency Representation of Multi-component Signals using Exponential Kernels. IEEE Trans. on ASSP, June, 1989
- 3 W. J. Williams and J. Jeong., "Reduced Interference Time-frequency Distributions," ISSPA Conf. and 1st Intl. Workshop on Time-Frequency Analysis and Its Applications, Gold Coast QLD, Australia, August, 1990.
- 4 P. Flandrin, "Some Features of Time-Frequency Representations of Multi-component Signals," IEEE Intl. Conf on ASSP, vol 3, pp. 41B.4.1-41B.4.4, 1984
- 5 F. Hlawatsch, "Interference Terms in the Wigner Distribution," in: Digital Signal Processing -84. V. Cappellini and A. Constantinides (eds), pp. 363-367, North-Holland, 1984
- 6 W. A. Watkins. "The Harmonic Interval: Fact or Artefact in Spectral Analysis of Pulse Trains," Marine Bio-acoustics, vol. 2., pp. 15-43, 1966.

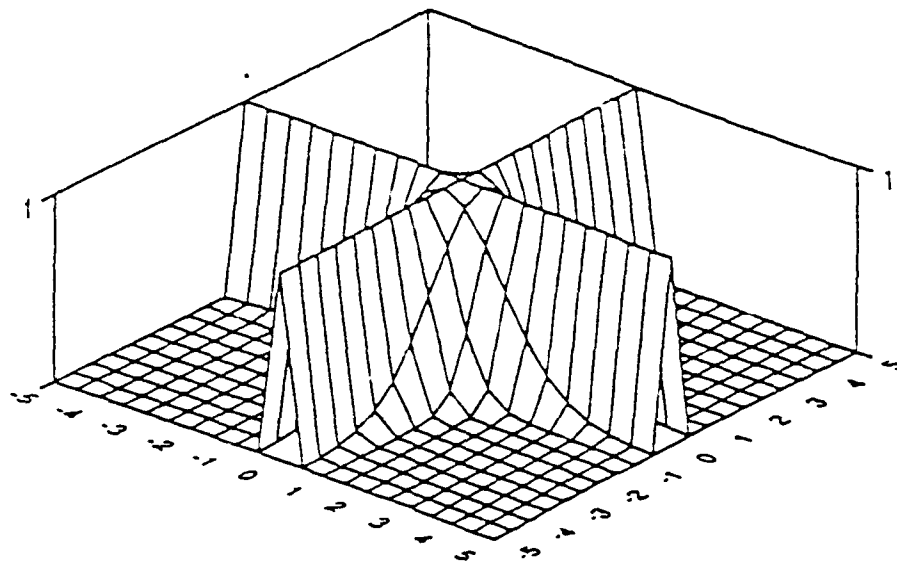
- P0. nonnegativity : $\rho_z(t, f; g) \geq 0 \forall t, f$
 Q0. $g(v, \tau)$ is the ambiguity function of some function $w(t)$.
 P1. realness : $\rho_z(t, f; g) \in \mathbb{R}$
 Q1. $g(v, \tau) = g^*(-v, -\tau)$
 P2. time shift : $s(t) = z(t - t_0) \Rightarrow \rho_s(t, f; g) = \rho_z(t - t_0, f; g)$
 Q2. $g(v, \tau)$ does not depend on t .
 P3. frequency shift : $s(t) = z(t)e^{j2\pi f_0 t} \Rightarrow \rho_s(t, f; g) = \rho_z(t, f - f_0; g)$
 Q3. $g(v, \tau)$ does not depend on f .
 P4. time marginal : $\int W_z(t, f) df = z(t)z^*(t)$
 Q4. $g(v, 0) = 1 \forall v$
 P5. frequency marginal : $\int \rho_z(t, f; g) dt = Z(f)Z^*(f)$
 Q5. $g(0, \tau) = 1 \forall \tau$
 P6. instantaneous frequency : $\frac{\int f \rho_z(t, f; g) df}{\int \rho_z(t, f; g) df} = f_i(t)$
 Q6. Q4 and $\frac{\partial g(v, \tau)}{\partial \tau} \Big|_{\tau=0} = 0 \forall v$
 P7. group delay : $\frac{\int t \rho_z(t, f; g) dt}{\int \rho_z(t, f; g) dt} = \tau_g(f)$
 Q7. Q5 and $\frac{\partial g(v, \tau)}{\partial v} \Big|_{v=0} = 0 \forall \tau$
 P8. time support : $z(t) = 0$ for $|t| > t_c \Rightarrow \rho_z(t, f; g) = 0$ for $|t| > t_c$
 Q8. $\psi(t, \tau) \triangleq \int g(v, \tau) e^{-j2\pi v t} dv = 0$ for $|\tau| < 2|t|$
 P9. frequency support : $Z(f) = 0$ for $|f| > f_c \Rightarrow \rho_z(t, f; g) = 0$ for $|f| > f_c$
 Q9. $\int g(v, \tau) e^{j2\pi f \tau} d\tau = 0$ for $|v| < 2|f|$
 P10. Reduced Interference
 Q10. $g(v, \tau)$ is a 2-D low pass filter type.

Table 1: Distribution properties and associated kernel requirements.

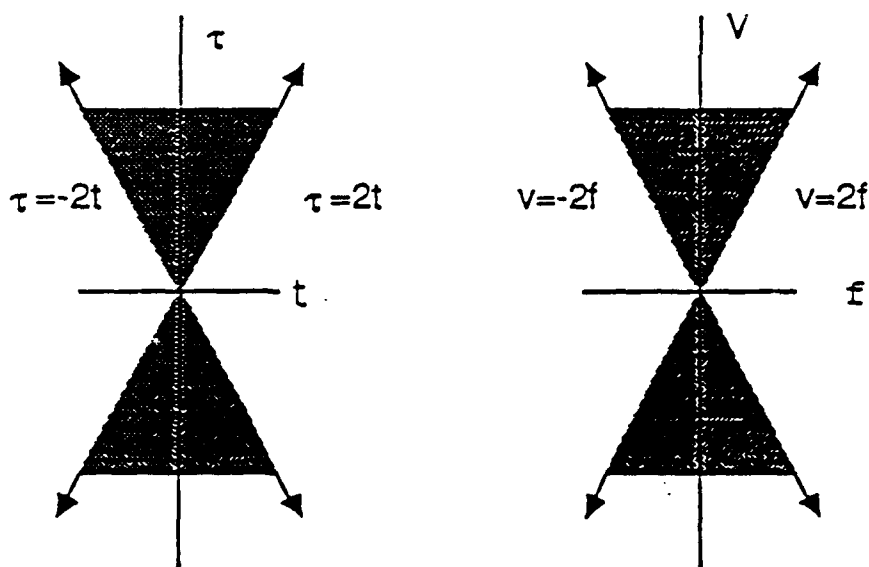
Distribution	$g(v, \tau)$	P0	P1	P2	P3	P4	P5	P6	P7	P8	P9	P10
Wigner	1		x	x	x	x	x	x	x	x	x	x
Rihaczek	$e^{j\pi v \tau}$			x	x	x	x				x	x
Re{Rihaczek}	$\cos(\pi v \tau)$		x	x	x	x	x	x	x	x	x	x
Exponential (ED)	$e^{-v^2 \tau^2 / \sigma}$		x	x	x	x	x	x	x			x
Spectrogram	$A_w(v, \tau)$ of a window $w(t)$	x	x	x	x	x						x
Born-Jordan*	$\frac{\sin(\pi v \tau)}{\pi v \tau}$		x	x	x	x	x	x	x	x	x	x
Windowed-ED*	$e^{-v^2 / \sigma} * W(v) \Big _{v=v\tau}$		x	x	x	x	x	x	x	x	x	x

* belongs to the RID.

Table 2: Comparison among several distributions.

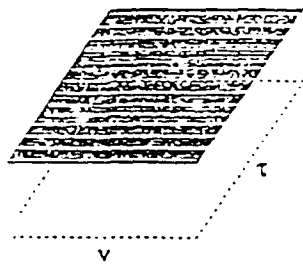


RID kernel $g(v, \tau)$

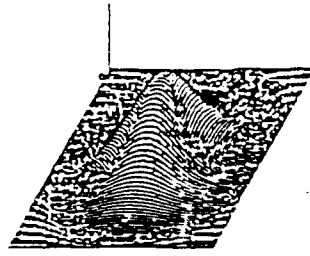


RID kernel Requirements for Time and Frequency Support

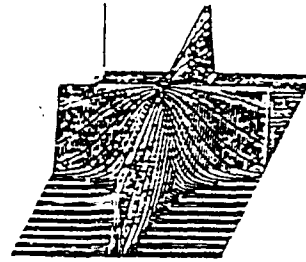
Essential Reduced Interference Distribution Requirements



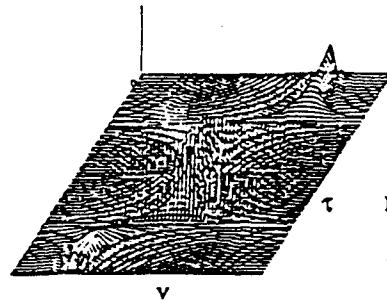
(a)



(b)



(c)

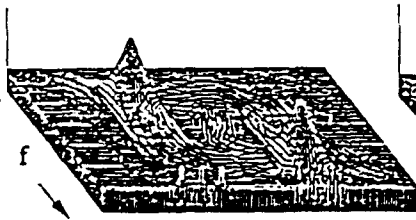


(d)

Figure 1a.-1c. Kernels of different distributions :
a. WD, b. spectrogram, c. RID

Figure 1d. Ambiguity function for signal in Figure 1c

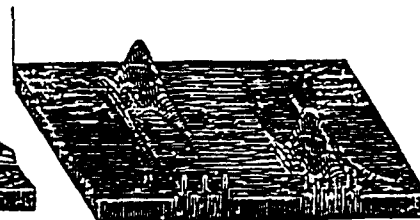
Figure 1e.-1g. t-f distributions for two sinusoids :
e. WD, f. spectrogram, g. RID



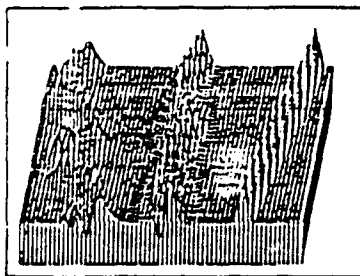
(e)



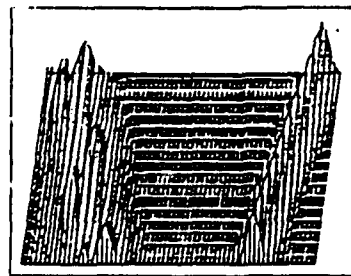
(f)



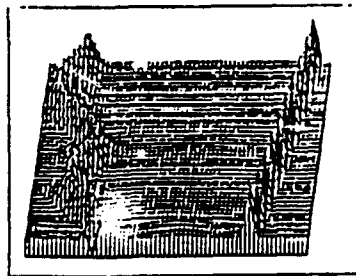
(g)



a. Wigner Distribution (WD)

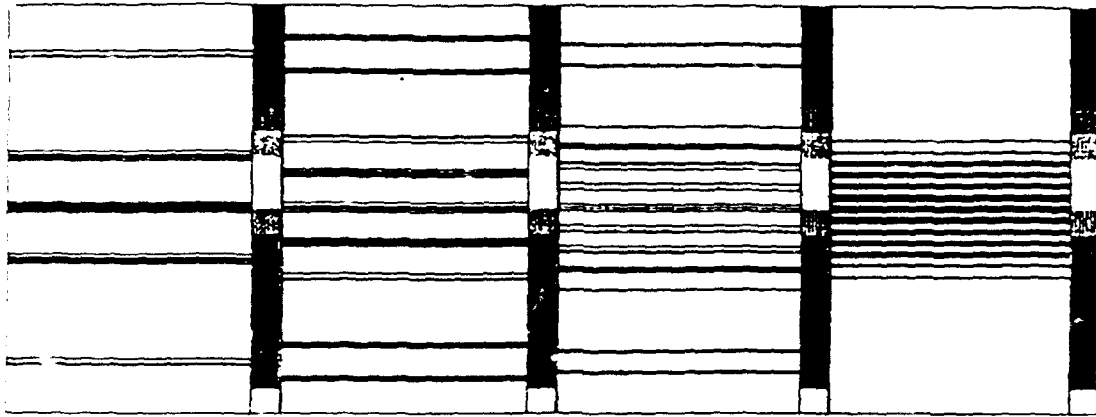


b. Spectrogram

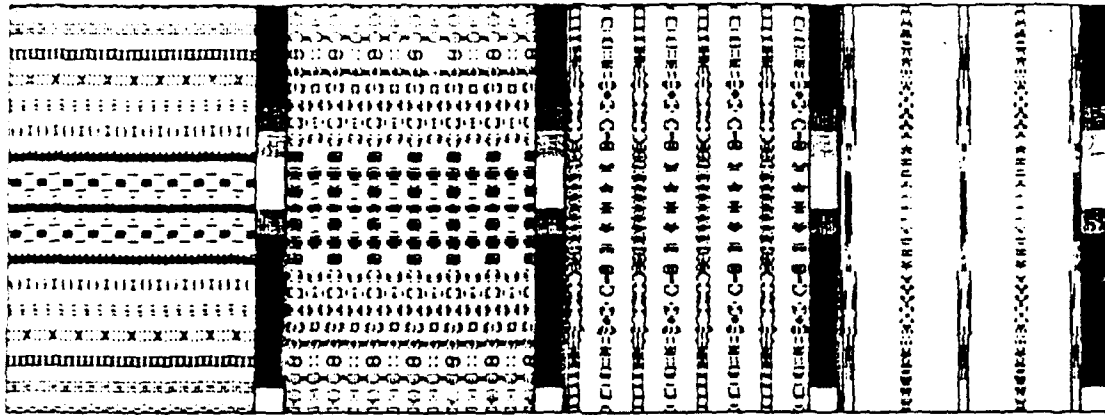


c. Reduced Interference Distribution

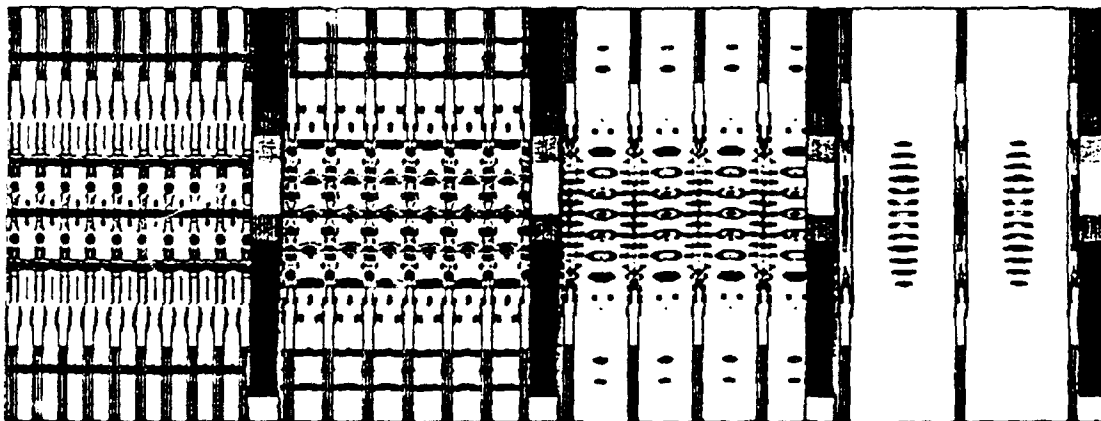
Figure 2. t-f distributions for a chirp plus FM signal:
a. WD, b. spectrogram, c. RID



(a)



(b)



(c)

FIGURE 3. A simulated sinusoid is pulsed 2 cycles on, 2 cycles off; 2 cycles on, 4 cycles off; 2 cycles on, 8 cycles off; 2 cycles on, 16 cycles off for the (a) spectrogram, (b) Wigner distribution, and (c) RID. The analysis window length is 256 points in all cases.

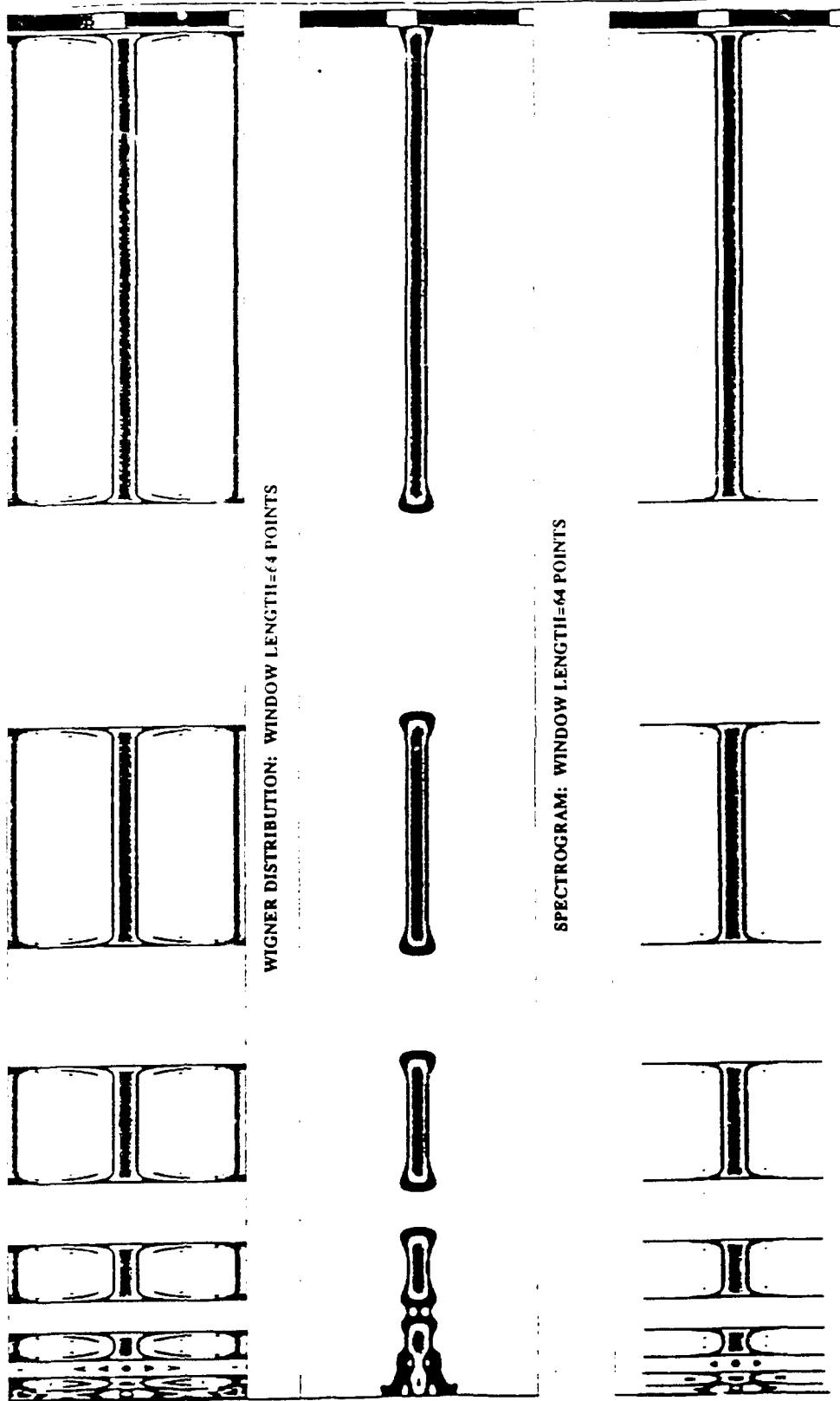
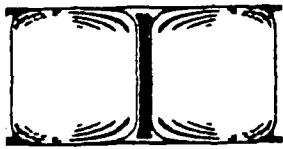
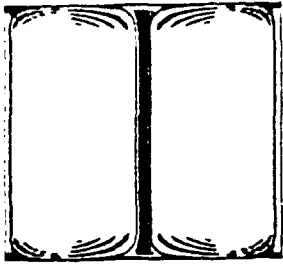
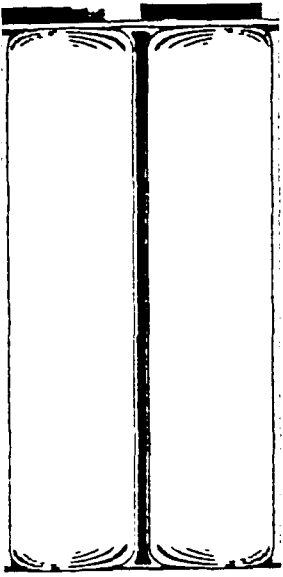
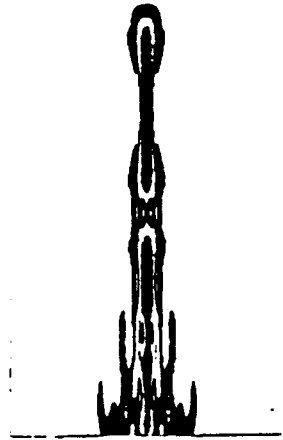
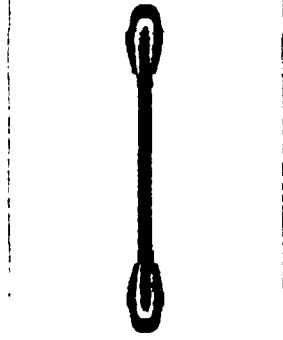
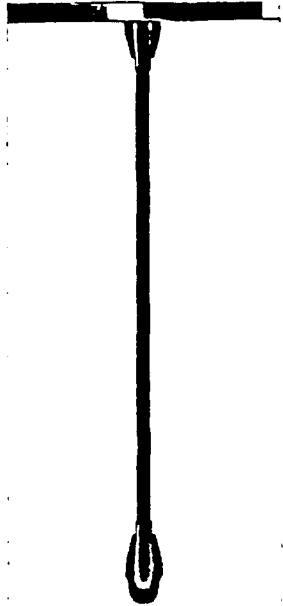


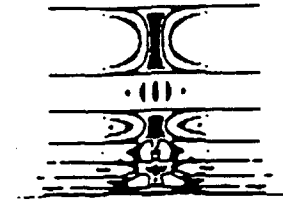
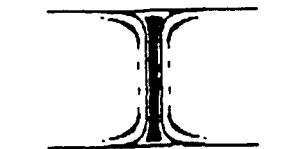
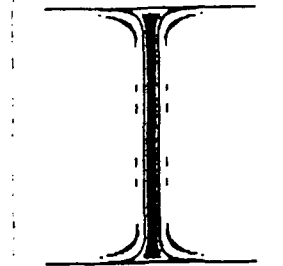
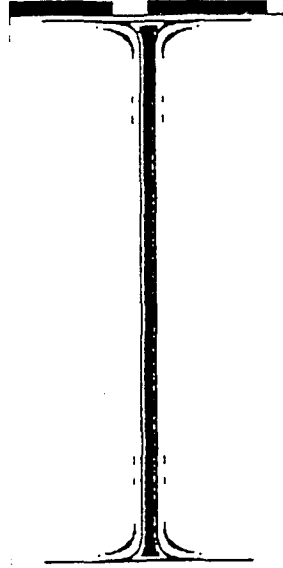
FIGURE 4a.



WIGNER DISTRIBUTION: WINDOW LENGTH=128 POINTS

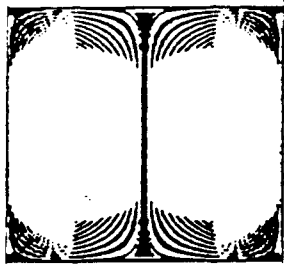
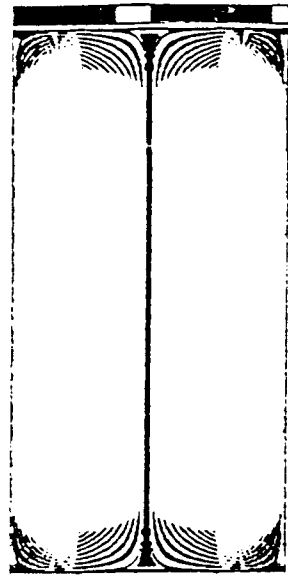


SPECTROGRAM: WINDOW LENGTH=128 POINTS

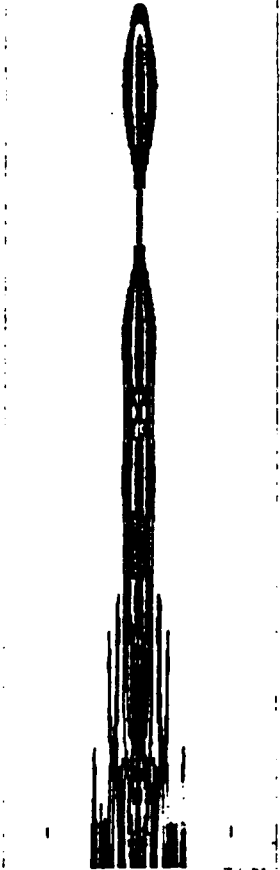
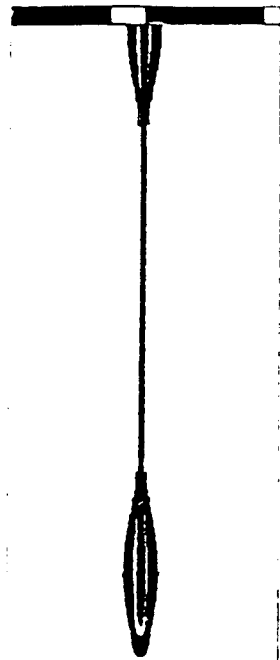


RID: WINDOW LENGTH=128 POINTS

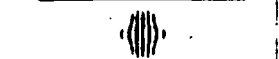
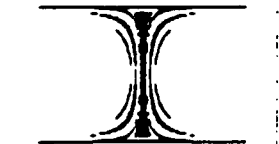
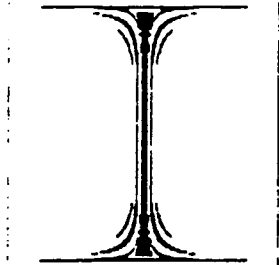
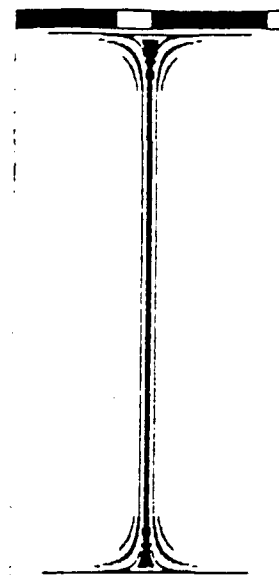
FIGURE 4b.



WIGNER DISTRIBUTION: WINDOW LENGTH=256 POINTS



SPECTROGRAM: WINDOW LENGTH=256 POINTS



RID: WINDOW LENGTH=256 POINTS

FIGURE 4c.

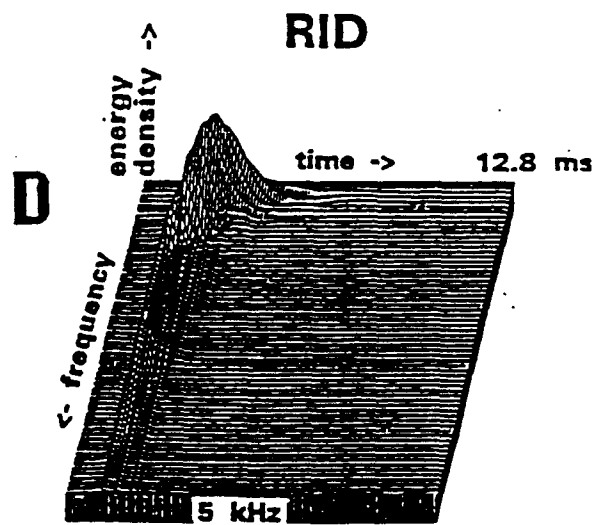
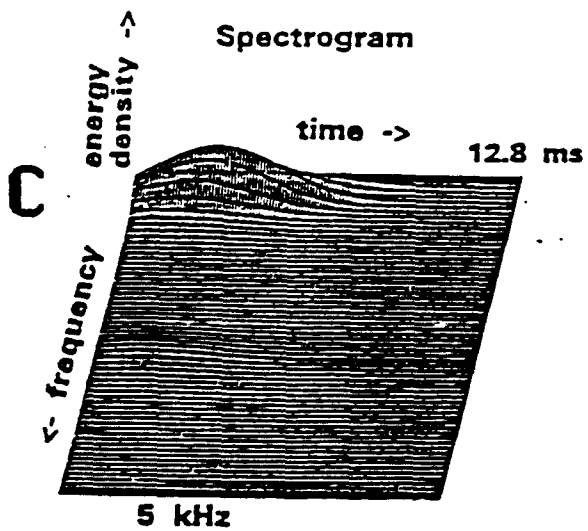
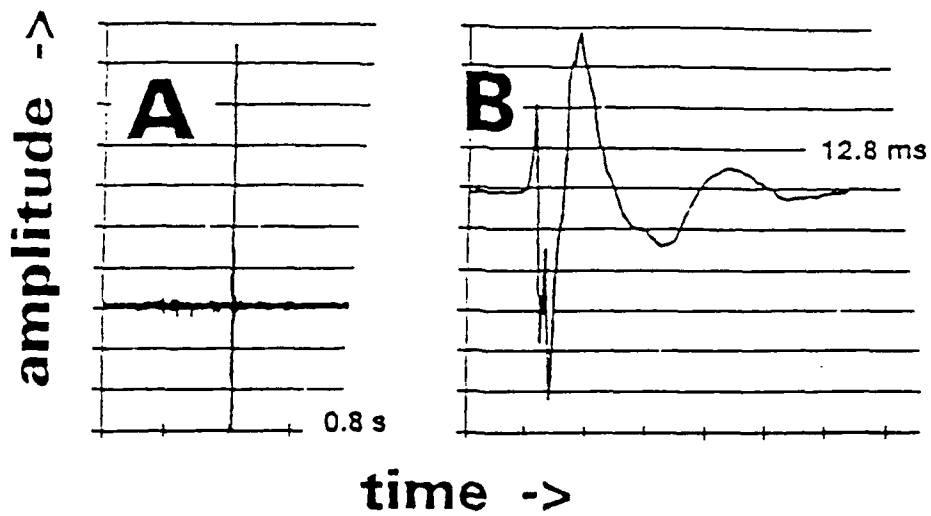


FIGURE 5. TEMPOROMANDIBULAR (JAW) JOINT CLICK

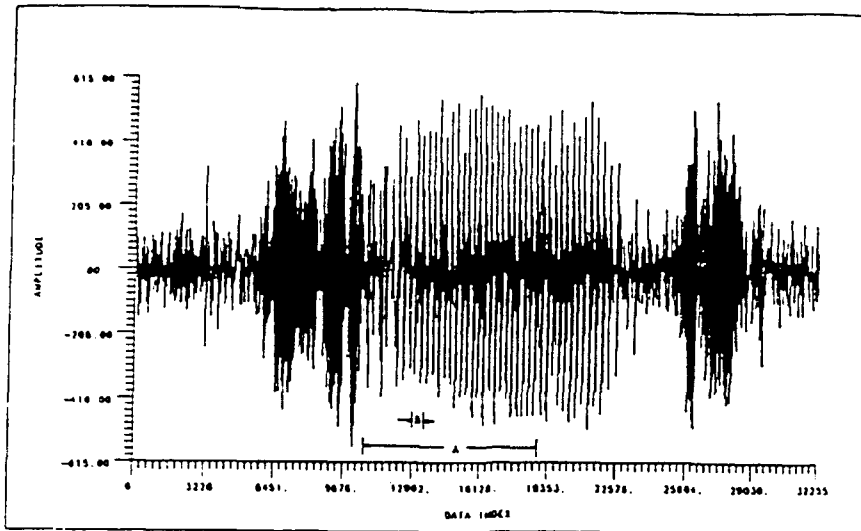


Figure 6a: Sectioned dolphin sound for 32256 samples (1.61 seconds)
 (Delimiters show areas expanded in Figure 6b. and 6c.)



Figure 6b: KED result of Figure 6a., area A

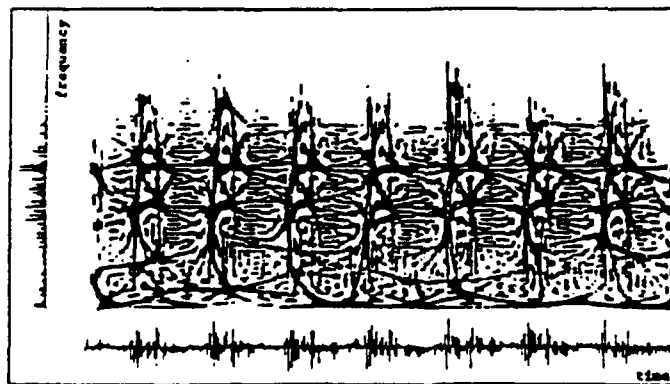


Figure 6c: KED result of Figure 6a., area B, superimposed
 with time series and Fourier spectrum

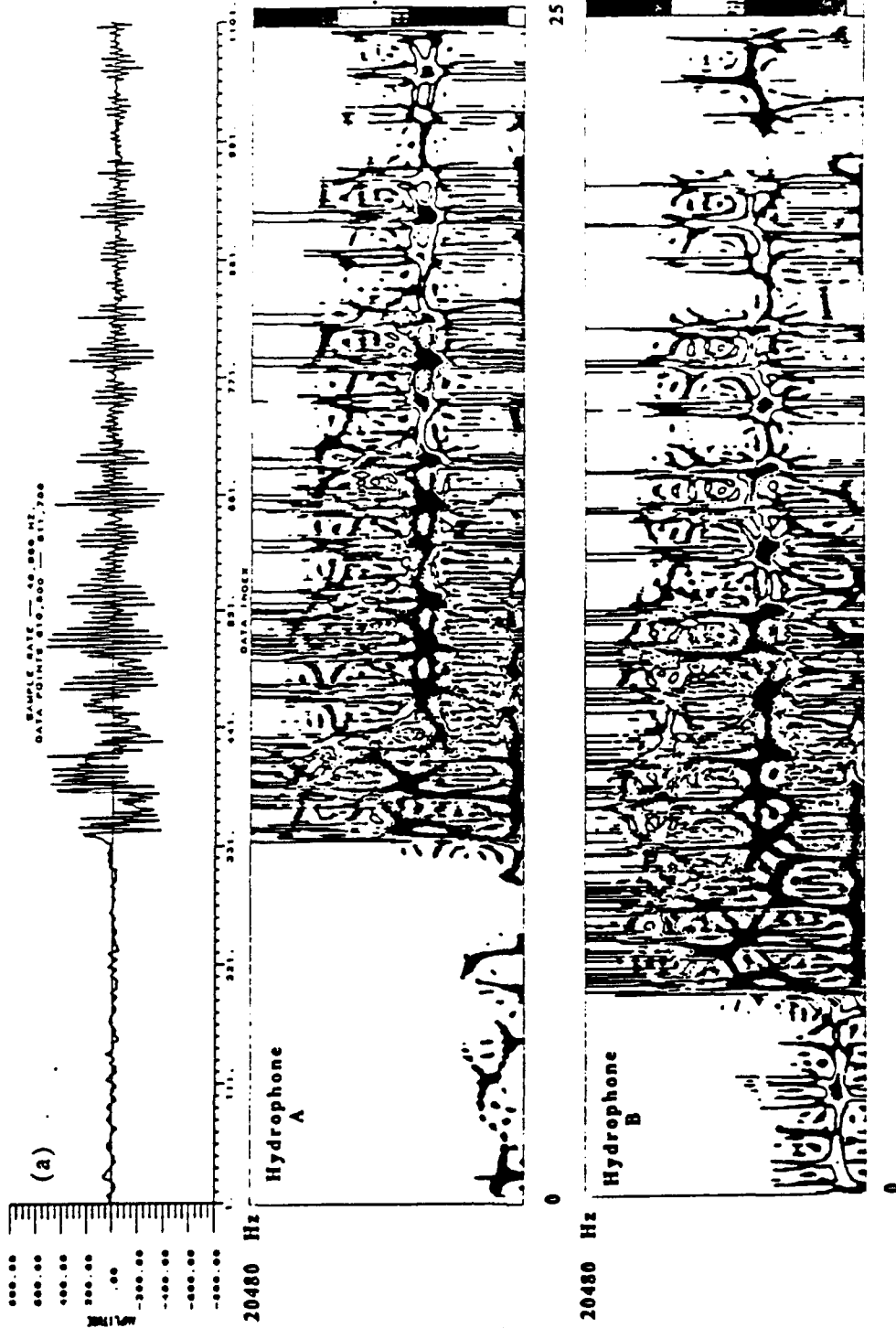


Fig. 7. One click of a five click sperm whale coda. 1100 point time sequence. The time series of the acoustic signal obtained at the first hydrophone is shown in (a). The RID result is shown for this time series in (b). The RID result for the second hydrophone is shown in (c). A 128 point analysis window was used with a sampling rate of 40,960 Hz.